The Journal of the Korean Society of
Coastal and Ocean Engineers
Vol. 4, No. 3, pp. 168~177, September 1992

On Tidal Energy Horizontal Circulation
潮汐에너지의 水平的 循環

Alexey V. Nekrasov*
알렉세이 네크라소프*

Abstract □ Some features of tidal energy horizontal flux in the ocean are considered, using the concept of "energy flux ellipses" which is a hodograph of momentary fluxes over a tidal semi-period. A number of characteristics of this ellipse are considered as well as some peculiarities of energy flux field in different types of tidal waves and their combinations (plane, Kelvin, Sverdrup, Poincare, amphidromic system). For forced tidal waves in equatorial channels some results are obtained explaining the dependence of energy flux direction on the channel dimensions.

要 旨 : 海洋에서의 潮汐에너지의 水平的循環에 대한 樣相은 半潮汐週期를 통한 瞬間플럭스의 軌跡인 "에너지 플럭스 楕圓"의 槪念을 적용하여 敍述하였다. 이 楕圓의 特性과 여러 形態의 潮汐波(平面, Kelvin, Sverdrup, Poincare 및 無潮點)體系에서의 에너지플럭스場의 特性이 考慮되었다. 赤道 또는 緯度에 平行한 水路에서의 强制潮汐波는 여러 水路諸元에서의 에너지플럭스 方向에 從屬됨을 說明하였다.

1. HORIZONTAL TIDAL ENERGY FLUX

The local horizontal flux of tidal energy is closely related with the wave nature of tidal movements and is characterized by its surface density $\vec{w}=\rho gh\xi\vec{u}$ in which ρ is sea surface density, g - gravity, h - depth, ξ - tidal surface elevation, $\vec{u}$ - vertically averaged tidal current velocity vector with comonents u and v. In general, for one tidal harmonic constituent one can write

$$\begin{aligned}\xi&=H\ \cos(\sigma t-\phi);\\ u&=U\ \cos(\sigma t-\phi_u);\\ v&=V\ \cos(\sigma t-\phi_v),\end{aligned}\qquad(1)$$

where H, U, V are amplitudes, ϕ, ϕ_u, ϕ_v are phases, σ is tidal frequency, t is time. If the tidal current is reversing (rectilinear), v vanishes and we obtain $w=w_a+w_r$, where

$$\begin{aligned}w_a&=(1/2)\rho ghHU\cos\beta[1+\cos2(\sigma t-\phi)];\\ w_r&=(1/2)\rho ghHU\sin\beta\sin2(\sigma t-\phi).\end{aligned}\qquad(2)$$

Here w_a, w_r are active (pulsating) and reactive (alternating) parts of w and $\beta=\phi_u-\phi$ is the phase shift between ξ and u (Godin, 1969). The w_a to w_r proportion in local tidal oscillation determines its structure indicating the proximity to either progressive or standing type. Both w_a and w_r oscillate with the frequency 2σ and their phase shift equals to $\pm 90°$. Time averaging of w gives zero for w_r and so the density of net energy flux is:

$$\langle w\rangle=\langle w_a\rangle=(1/2)\rho ghHU\cos\beta.\qquad(3)$$

If the tidal current is rotary (what is more common) and its hodograph is an ellipse, the vector $\vec{w}$ also changes its direction and has the components w_x and w_y each in general consisting of active and reactive parts as follows

$$\begin{aligned}w_{a,x}&=(1/2)\rho ghHU\cos\beta_x[1+\cos2(\sigma t-\phi)];\\ w_{r,x}&=(1/2)\rho ghHU\sin\beta_x\sin2(\sigma t-\phi);\end{aligned}\qquad(4)$$

$$\begin{aligned}w_{a,y}&=(1/2)\rho ghHV\cos\beta_y[1+\cos2(\sigma t-\phi)];\\ w_{r,y}&=(1/2)\rho ghHV\cos\beta_y\sin2(\sigma t-\phi).\end{aligned}\qquad(5)$$

where $\beta_x=\phi_u-\phi$ and $\beta_y=\phi_v-\phi$ are phase shifts of

*러시아水文氣象硏究所(Russian State Hydrometeorological Institute, St. Petersburg, Russia)

components u and v with respect to ξ. From Eqs. (4) and (5) one can see that the relations $w_{a,x}$: $w_{a,y}$ and $w_{r,x}$: $w_{r,y}$ do not depend on time, i.e. the directions of $\vec{w}_a$ and $\vec{w}_r$ remain constant and may be determined by the azimuths

$$\gamma_a = \tan^{-1}(w_{a,x}/w_{a,y}) = \tan^{-1}(U\cos\beta_x)/(V\cos\beta_y)]$$
$$\gamma_r = \tan^{-1}(w_{r,x}/w_{r,y}) = \tan^{-1}[(U\sin\beta_x)/(V\sin\beta_y)]. \quad (6)$$

Comparison of Eq. (6) with Eq. (1) shows that the azimuth γ_a coincides with direction of the current for the moment $t_{HW} = \phi/\sigma$ (high water) and the azimuth γ_r-with that for zero level moment $t_z = t_{HW} \pm T/4$ ($T = 2\pi/\sigma$ is tidal period). Time averaging of $\vec{w}$ again gives zero for $\vec{w}$ and for the density of net energy flux one obtains

$$\langle\vec{w}\rangle = (1/2)\rho g h H \vec{u}_{HW}, \quad (7)$$

where $\vec{u}_{HW}$ is the current vector for the moment of high water.

The behaviour of $\vec{w}$ in time can be described by a "fan-like" variation of a vector issuing from given origin point. The hodograph of this vector forms an ellipse geometrically similar to that of tidal current Nekrasov, 1987. Both the ellipses have the same oblateness and orientation, and it is convenient to depict them simultaneously with coinciding origin points (Fig. 1). In this case the line segment connecting the centers of current and flux ellipses correcponds in direction (and also in value, if the scale accepted for w is used) with the net flux vector $\langle\vec{w}\rangle$. The $\vec{w}$-vector runs round the flux ellipse twice per one tidal period T, whereas the $\vec{u}$-vector performs only one complete revolution per T. On the whole the simultaneous representation of both ellipses may be used as an energetically informative diagram.

In general the horizontal energy flux provides the transfer of tidal energy from sources to sinks. This transfer is realized in form of tidal waves which can be either free or forced determining, correspondingly, either induced (co-oscillating) or proper (independent) tide. It seems expedient to consider some characteristic features of the horizontal energy circulation by application of $\vec{w}$-diagrams to commonly known analytical solutions describing different types of tidal waves. Various examples of such diagrams are shown below.

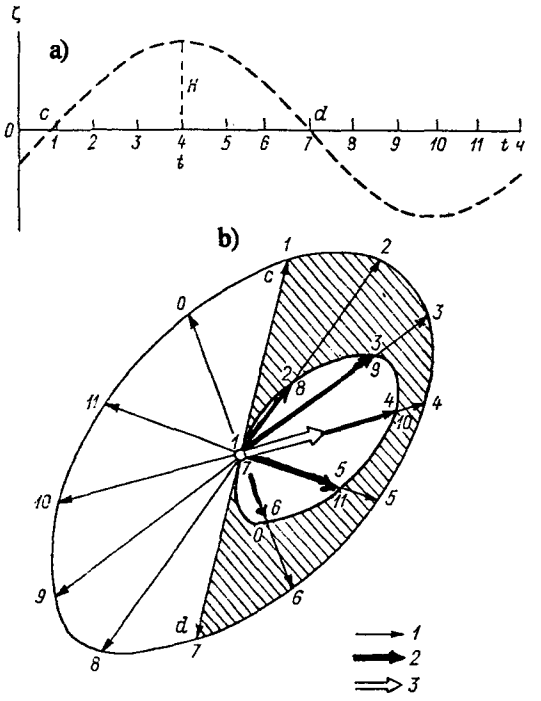

Fig. 1. Construction of energy vector diagram.
a) tidal oscillations of sea susface; b) tidal current ellipse and corresponding hodograph of $\vec{w}$-vector (energy flux ellipse).
1-hourly corrent vectors, 2-hourly $\vec{w}$-vectors, 3-net flux vector $\langle\vec{w}\rangle$.

2. PLANE WAVES

For individual plane tidal wave the $\vec{w}$-diagrams have rectilinear form in accordance with reversing character of tidal currents. In Fig. 2 the $\vec{w}$-diagrams for free progressive, standing and intermediate (progressive-standing) waves are given corresponding to purely active, purely reactive and mixed type of energy fluxes. If a is the amplitude of positevely directed wave and b is that of negatively directed one, k being their wavenumber, so for three mentioned cases one obtains for w:

$$w_p = (1/2)M[1+\cos2(\sigma t - kx)];$$
$$w_s = M\ \sin2kx\ \sin2\sigma t; \quad (8)$$
$$w_{ps} = (1/2)M(1-r^2)[1+\cos2(\sigma t - kx)] + M\,r^2 \sin2kx \cdot \sin2\sigma t,$$

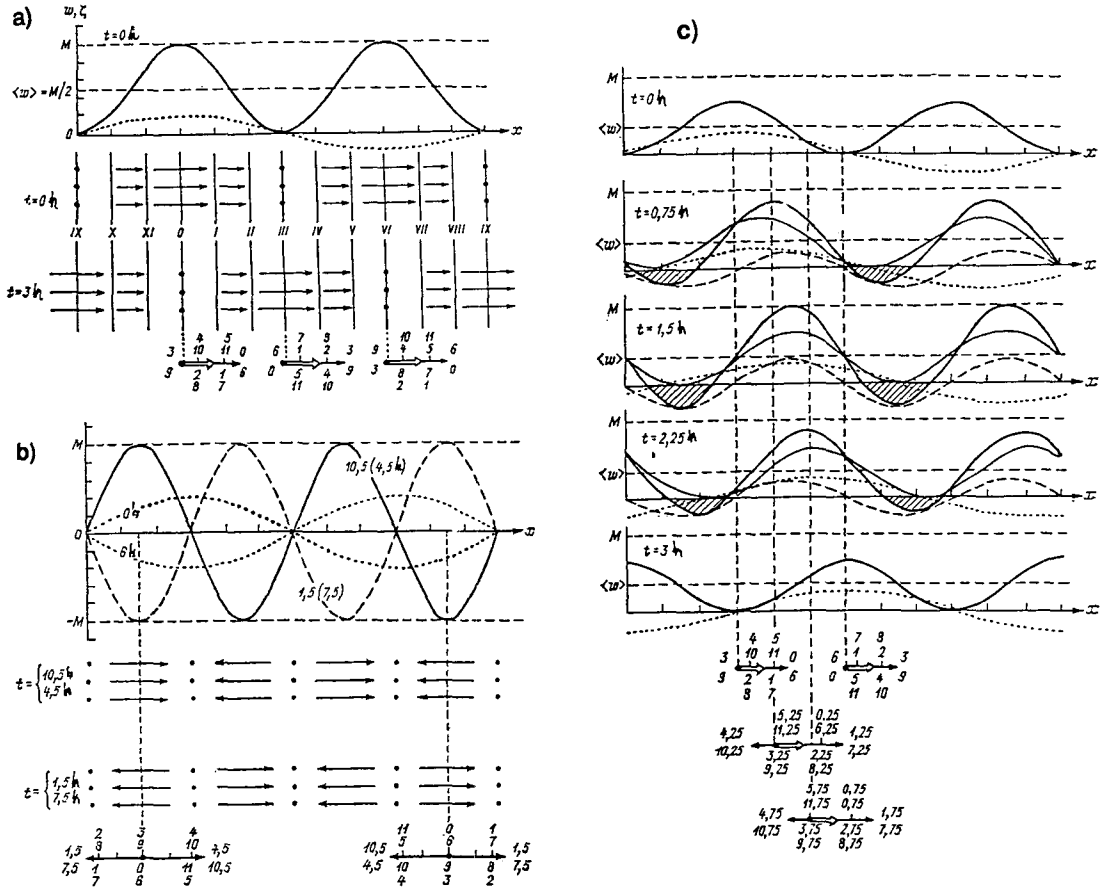

Fig. 2. Energy flux in plane waves.
a) Purely active energy flux (solide curve) in plane progressive wave at the moment t=0. Dotted curve-sea surface profile vector filed for $\vec{w}$ are given for two moments. Cotidal lives are also shown. For points lying on cotidals 0, III and VI the energy vector diagrams (here rectilinear) are depicted; b) Energy flux in plane standing wave for four moments (t=1.5; 4.5, 7.5 and 10.5). Fluxes are reactive and equal to zero for nodes and antinodes, being maximal at half way between them; c) Active (thin), reactive (broken) and summary (thick) flux density distribution in progressive-standing wave with r=0.577 for various moments. By dotted line the "progressive past" of the mixed wave for relevant moments is shown. Energy vector diagrams for some points are given in the bottom.

and

$$\begin{aligned} \langle w_p \rangle &= (1/2)\ M; \\ \langle w_s \rangle &= 0; \\ \langle w_{ps} \rangle &= (1/2)\ M(1-r), \end{aligned} \tag{9}$$

where $M=\rho g\, a^2\sqrt{gh}$. Only for progressive wave the vector field of net fluxes is spacely uniform; in other cases it is attenuated in nodes and antinodes and is amplified at half way between them.

The elliptic form is acquired by $\vec{w}$-diagram in case of cross-intersection of plane waves. In particular but important case of crossing of two standing waves, the so-called "Harris amphidromies" arise with cotidal lines pattern resembling a system of gears staggerly meshed and forming cells of rhombic form with alternating sign of phase gyration (Fig. 3). The tidal currents become rotating the sense of rotation corresponding to that of phase giration. Geometric details of resulting picture depend on the amplitude and phase relationship of partial waves superposed and the angle of their intersection. In Fig. 4 the $\vec{w}$-diagrams for two contiguous

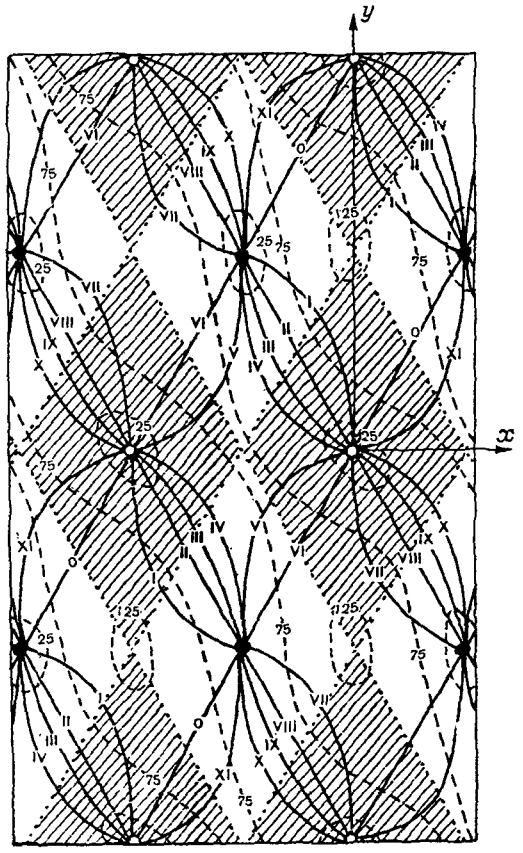

Fig. 3. Amphidromic systems ("Harris amphidromies") resulting from cross-interference of two plase standing waves with $n_s=0.6$; $\alpha=60°$ and $\psi=60°$ (2 hours). The *rhombic* cells of right and left phase gyration are shown with covesponding amphidromic points (black or white) in their centers.

cells, "meshed" with their mutual cotidal lines, are shown. One can see that though the current and flux ellipses (and so the instantaneous energy fluxes) are different in right and left cells, the net flux patterns in these cells are bilaterally symmetric. The components of net flux are determined as follows:

$$\langle w_x\rangle = -2M\ n_s\ sin\alpha\ sin\psi\ sin2k''y;$$
$$\langle w_y\rangle = 2M\ n_s\ cos\alpha\ cos\psi\ sin2k'x, \qquad (10)$$

where n_s is the amplitude ratio of crossing standing waves, α is semi-angle of their intersection, ψ is the phase difference of these waves, and k', k'' are projections of wavenumber vector $\vec{k}$ on axes x and

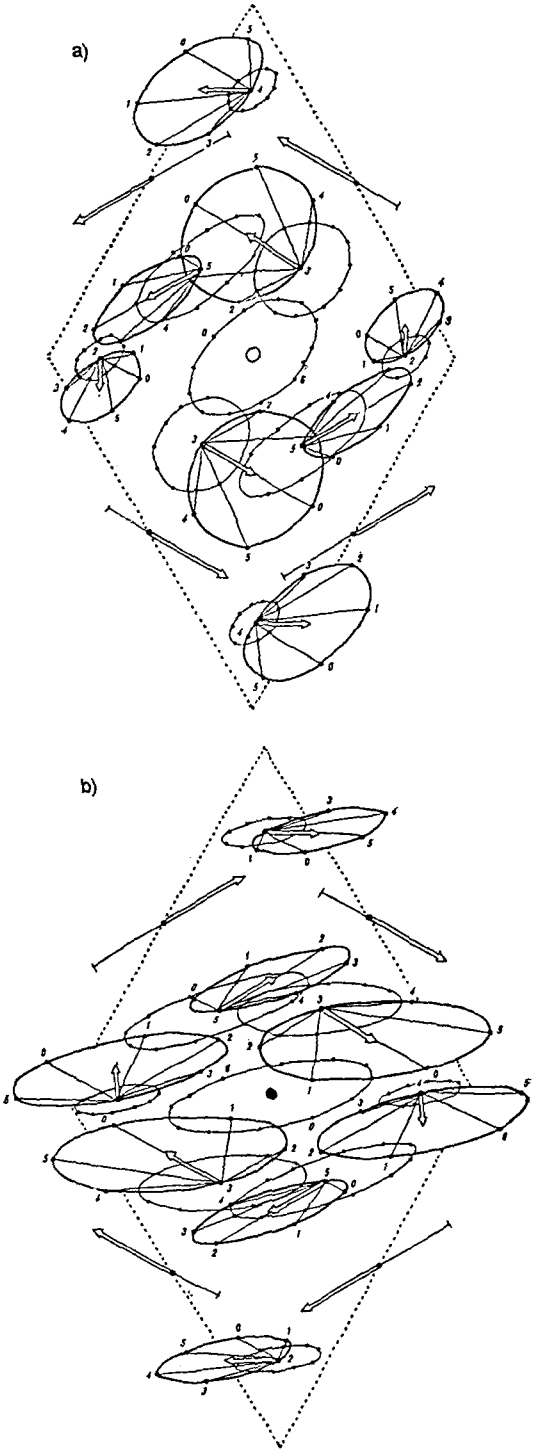

Fig. 4. Current (thin) and energy flux (thick) ellipses in two contiguous cells. Instentaneous fluxes are different in these cells but net fluxes (broad open arrows) are bilaterally symmetric.

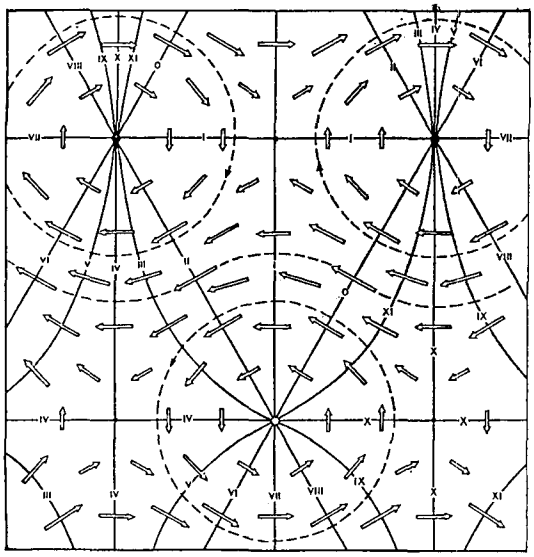

Fig. 5. Net fluxes in "Harris amphidromies" with: $n_r=1.0$; $\alpha=60°$, $\psi=60°$.

y, i.e. $k'=k\sin\alpha$; $k''=k\cos\alpha$. Generally net flux vectors are represented by alternating closed circulations around amphidromic points with intensity being maximal as the phase shift between crossing waves approaches to $\pm 90°$ (Fig. 5).

3. KELVIN WAVES

Though the Coriolis force, being inertial, does not do any work and does not change the total tidal wave energy content, its effect leads to significant transform of kinematic characteristics and energy structure of a wave.

The most common analytical solutions describing tidal waves in presence of the Coriolis force are given in form of the Kelvin, Sverdrup and Poincaré waves. For the Kelvin wave we have

$$w_k=(1/2)\ M_k\ [1+\cos 2(\sigma t-kx)];$$
$$\langle w_k\rangle=(1/2)\ M_k, \qquad (11)$$

where $M_k=\rho g\, a_k^2\sqrt{gh}$. Here $a_k=a(mB/\sinh mB)\cdot\exp(-my)$-is the Kelvin wave amplitude, B is the width of the basin, $m=f/\sqrt{gh}$ (where f is the Coriolis parameter) and a is the amplitude of "E-equivalent" (equivalent in energy content) plane wave. In Fig. 6 some characteristics of energy flux in Kelvin

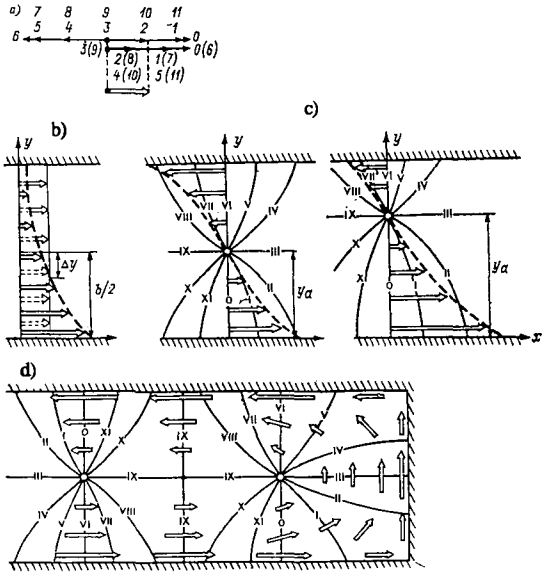

Fig. 6. Energy fluxes in Kelvin waves.
a) Energy vector diagram for a semi-diamal cycle;
b) Energy flux profile across the channel for Kelvin and E-equivalent plane waves; 3) Energy flux profiles for interference of two opposite Kelvin waves having equal (left) and nonequal (right) amplitudes;
d) Scheme of energy cross-transfer following the Kelvin wave reflection in a rectangular bay.

waves are presented which are determined primarily by energy concentration in the right (in the Northern Hemisphere) flank of an individual wave with corresponding local intensification of the energy flux (the $\vec{w}$-diagram remaining rectilinear). The interference of two opposite Kelvin waves in a channel-like basin of width B may lead to the rise of "Taylor amphidromies" and to "energetic countercurrent" near one of channel sides if the amplitude ratio of waves exceeds $\exp(-fB/gh)$. If a Kelvin wave reflects in the head of a gulf, the superposition of arising standing Poincaré waves provides the transfer of energy across the gulf completing the contrary fluxes by a "transversal link". Note that in contrast with abovementioned "Harris amphidromies" there is no closed energy circulations around those of Taylor.

4. SVERDRUP AND POINCARÉ WAVES

For a progressive Sverdrup wave travelling in x-

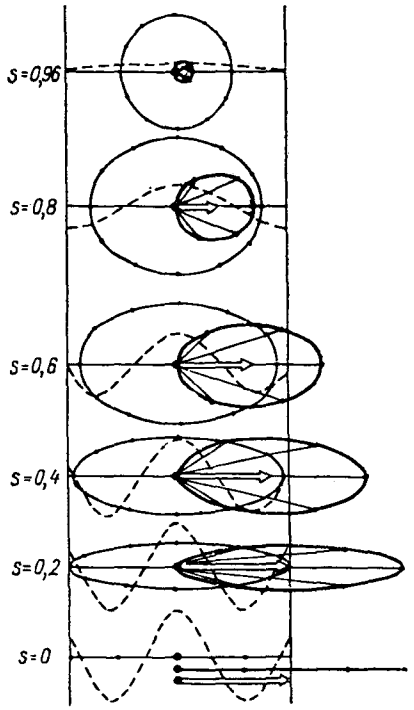

Fig. 7. Current and energy flux ellipses in Sverdrup waves for different S. with broken curve the wave profile is schematically shown.

direction we have

$$w_x=(1/2)\ M_s\ [1+\cos 2(\sigma t-k_s x)];$$
$$w_y=(1/2)\ s\ M_s \sin 2(\sigma t-k_s x); \tag{12}$$

$$\langle w_x\rangle=(1/2)\ M_s;$$
$$\langle w_y\rangle=0, \tag{13}$$

where $M_s=\rho\ g\ a_s^2(1-s^2)^{-1/2}\sqrt{gh}$. Here $a_s=a(1-s^2)^{3/4}$ is the amplitude of Sverdrupe wave, $k_s=k(1-s^2)^{1/2}$ is the wavenumber of the Sverdrup wave and $s=f/\sigma$. As in the case of Kelvin wave, a is the amplitude of "E-equivalent" plane wave. In Sverdrup waves the equality of potential and kinetic energies is violated in favour of the latter and here the $\vec{w}$-diagrams become elliptic and depend substantially on the parameter s (Fig. 7). The longitudinal flux component is purely active whereas the transversal component is purely reactive. The net flux is spacely uniform and depends inversely on s tending to zero when $s\to 0$ (at "critical" latitudes). If the Sverdrup wave reflects normally and totally from the shore, the

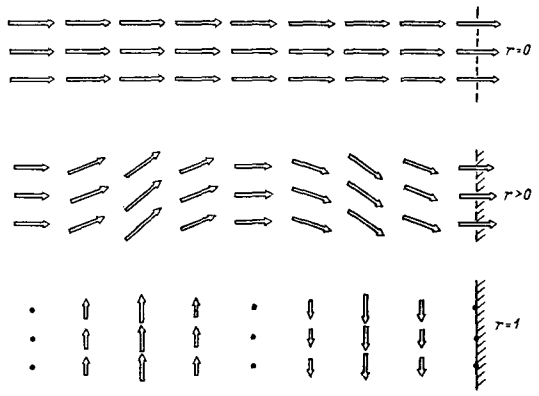

Fig. 8. Horirontal energy net fluxes for the zero, partial and total reflection of a Sverdrup wave from the straight coast.

$\langle\vec{w}\rangle$ vector field is divided into zones with net fluxes having contrary alongshore directions; if the reflection is not total, the net fluxes only deviate from the normal to the shore (Fig. 8).

If the reflection of Sverdrup wave is oblique, it results in progressive Poincaré wave travelling along the coast with the alongshore flux components being purely active and the normal to shore components-purely reactive. If the coastline is oriented along the x-axis, we have

$$w_x=M_s\ [\sin\alpha(1+\cos 2k''y)-s\ \cos\alpha \sin 2k''y]\ [1+\cos 2(\sigma t-k'x)];$$
$$w_y=M_s\ [\cos\alpha \sin 2k''y-s\ \sin\alpha(1+\cos 2k''y)]\ \sin 2(\sigma t-k'x); \tag{14}$$

$$\langle w_x\rangle=M_s\ [\sin\alpha(1+\cos 2k''y)-s\ \cos\alpha \sin 2k''y];$$
$$\langle w_y\rangle=0. \tag{15}$$

The net flux is directed along the shore and mainly with the wave. However, a specific effect takes place in this case constituting in formation of stripe-like alongshore zones with net flux directed opposite to the phase velocity of Poincaré wave (Nekrasov, 1987). Figs. 9 and 10 illustrate this effect and its dependence on distance from the shore, the parameter s and the angle of intersection of initial Sverdrup waves.

Taking into account the Coriolis force modifies the tidal energy circulation in "Harris amphidromies" resulting from cross-interference of standing

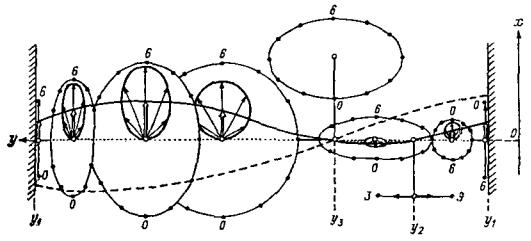

Fig. 9. Current and energy flux ellipses for a Poincaré wave in a channel-like basin. Solid curve - net flux cross-profile; broken curve - sea surface profile for t=0.

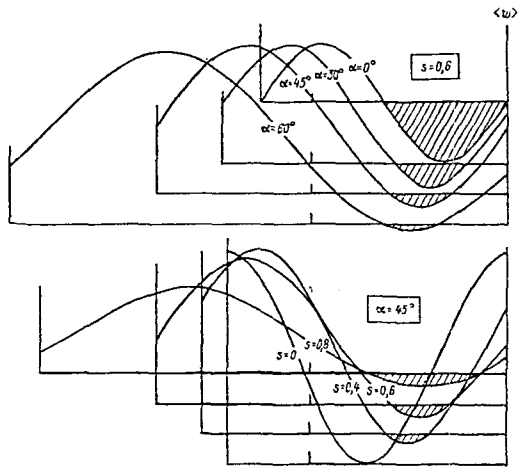

Fig. 10. Cross-profiles of net energy flux in a Paincaré wave for different α and s.

waves (Fig. 11). The principal effect consists in intensification of cum-sole (right, if s>0) circulation rings with weakening of contra solem (left, if s>0) ones. Similar results can be obtained by considering the reflection of progressive Poincaré waves in the head of a wide gulf-like basin. As it is shown in Fig. 12, such a reflection leads to intensive cum-sole energy circulation around the central "axial" amphidromic point accompanied by the relatively weak contra-solem circulation around the "coastal" amphidromies (Nekrasov, 1990). If the Poincaré wave reflection is total, one can say that the Coriolis force makes it possible to net fluxes to arise, but only in form not modifying the integral energy balance and tolerating nothing but closed circulations around amphidromies.

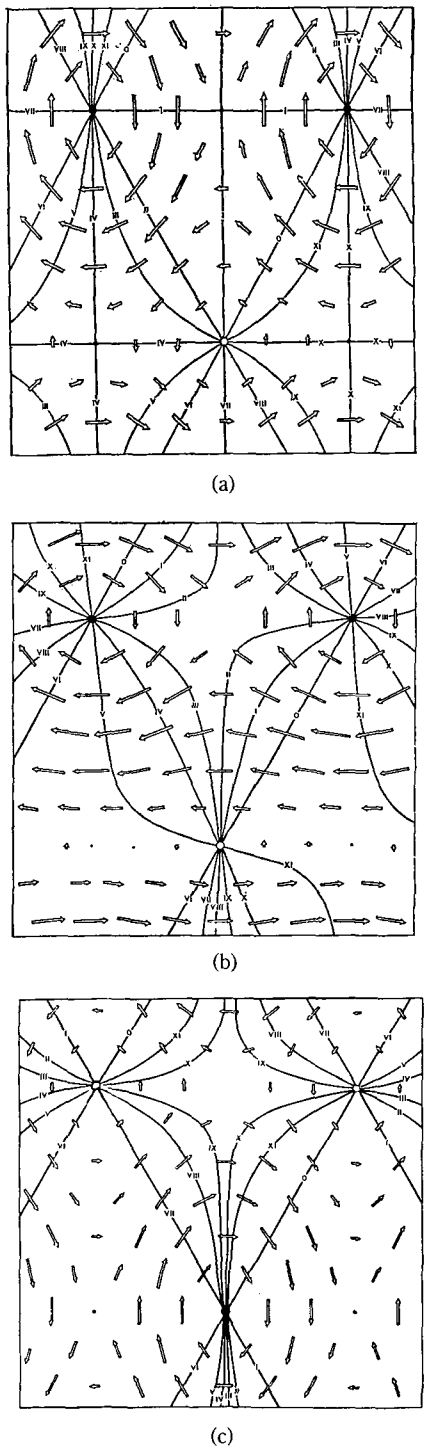

(a)

(b)

(c)

Fig. 11. Net fluxes in "Harris amphidromies" resulting from cross-interference of two standing Sverdrup waves with $n_1=1.0$, $\alpha=60°$, $s=0.519$ for different ψ. a) $\psi=60°$; b) $\psi=128°$; c) $\psi=210°$.

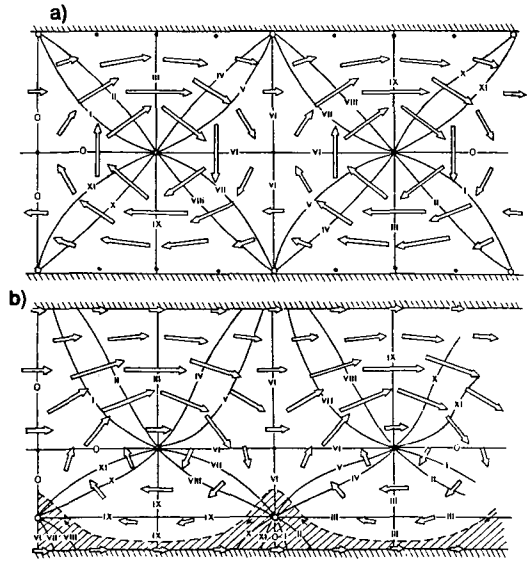

Fig. 12. Net fluxes resulting in a channel from reflection of Poincaré wave with $\alpha=45°$ and $s=0.7337$. a) total reflection ($r=1.0$); b) partial reflection ($r=0.5$)

5. ENERGY FLUX IN FORCED TIDAL WAVES

To analyse some specific characteristics of energy flux in forced tidal waves caused by direct action of tide-generating force, we shall confine ourselves to consideration of the simplest solutions for semi-diurnal tidal movements in channels of constant depth and width oriented along the equator or a latitude parallel. By varying the parameters of the channel one can imitate approximately the conditions typical for seas, gulfs, straits, shelves or, lastly, ocean basins.

The consideration of tidal energetics in basins of mentioned type can be started on the basis of solution obtained by H. Lamb and L. Swain (1915) for an equatorial channel enclosed on its ends and without friction. In this case, using the expressions for ξ and u given in Lamb and Swain (1915), we have for the net energy flux:

$$\langle w\rangle = -\{(\rho g\hat{H}^2R\sigma)/[4(q^2-1)^2]\}\,[1+(q\sin 4\alpha)/(\sin 4q\alpha) - A\cos 2q\lambda\cdot\cos 2\lambda + D\sin 2q\lambda\cdot\sin 2\lambda] \quad (16)$$

with

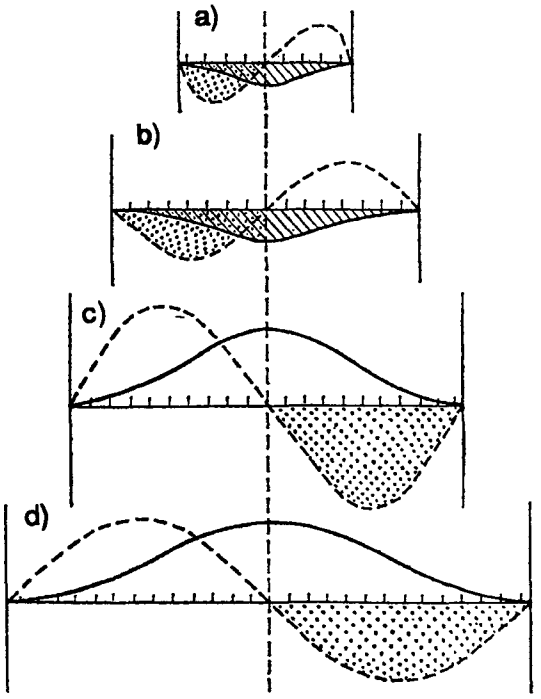

Fig. 13. Distribution of timely averaged densities of energy fluxes (solid curves) and work done by M_2 tide-generating force (broken curves) along the enclosed basins with different lengths ($h=3268$m): a) $L=2000$ km; b) $L=3500$ km; c) $L=4500$ km; d) 6000 km.

$$A=\cos 2\alpha/\cos 2q\alpha+q\sin 2\alpha/\sin 2q\alpha;$$
$$D=\sin 2\alpha/\sin 2q\alpha+q\cos 2\alpha/\cos 2q\alpha, \quad (17)$$

where $\hat{H}$ is the amplitude of equilibrium tide, R is the Earth's radius, $q=\sigma R/\sqrt{gh}$ and λ is the geographical longitude. The channel has its central point at $\lambda=0$ and its closed ends at $\lambda=\pm\alpha$. In this basin, with absence of dissipation and energy radiation, the energy budget is to be maintained by a work p done by tide-generating force, i.e. the action of astronomical sources and sinks, is to be balanced and must be accompanied by a net energy flux $\langle w\rangle$ directed from the formers to the latters. In Fig. 13 the distribution of net values $\langle p\rangle$ and $\langle w\rangle$ are presented along the basins of different depth and length showing the considerable dependence of mentioned net values on the basin geometry. If the basin length is relatively small (under the first resonance) the eastern half of the basin repre-

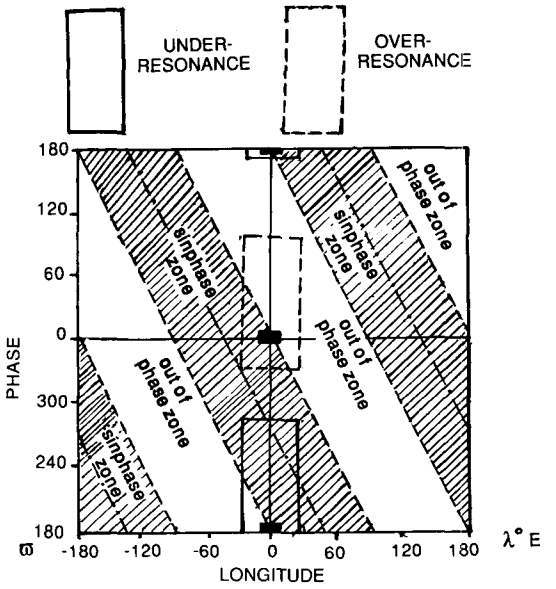

Fig. 14. Changes in astronomical source and sink positions for under-resonance and over-resonance situations.

sents the energy source and the western half is the sink the wave motion transporting energy from east to west (in negative direction). After passing the resonance (for longer basins) the situation changes: as a result of general inversion of the response phase the source and the sink change their places, and energy is now transported from west to east (Figs. 14 and 15).

Some generalization of these results may be achieved by introducing the "impedance" boundary conditions at the ends of mentioned channels what imitates partial radiation or "contour" dissipation of energy. For western (W) and eastern (E) ends these conditions may be written in the form:

$$\begin{aligned} &\text{for (W): } u = -[(1-r_W)/(1+r_W)]\cdot\xi\sqrt{gh}; \\ &\text{for (E): } u = [(1+r_E)/(1+r_E)]\xi\sqrt{gh}, \end{aligned} \qquad (18)$$

where r_W, r_E are amplitude coefficients of reflection, generally complex. In our case only real positive values of r are used imitating coastal dissipative losses.

Employment of Eq. (18) results in significant changes in the scheme of the energy budget by adding to it geophysical sinks, whose existence at, say, one of the ends leads to a "suction" of energy from

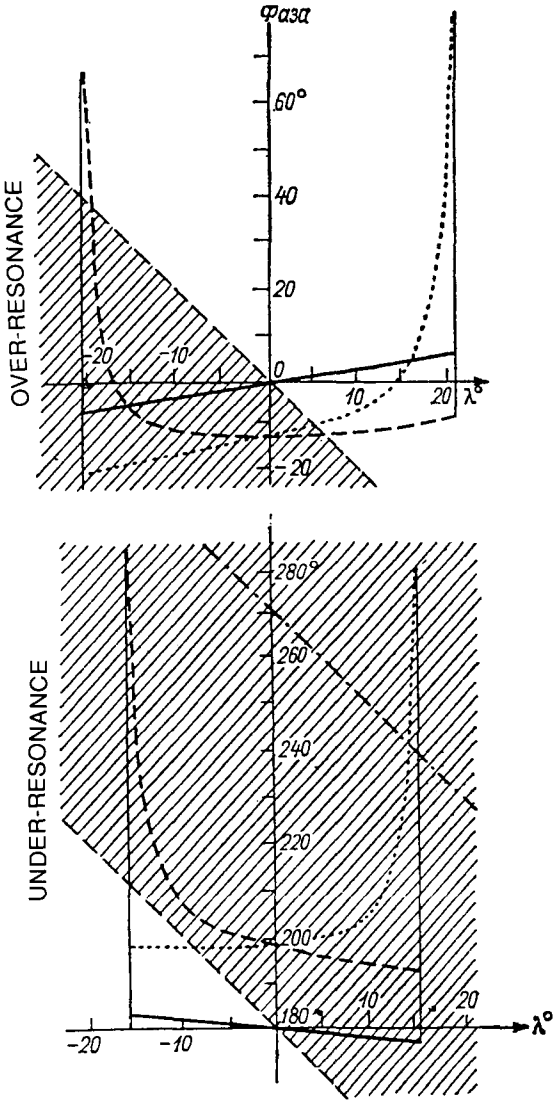

Fig. 15. Tidal current phase distribution along the equatorial channel-like basins for under- and over-resonant conditions corresponding to b) and c) in Fig. 13. solid curves: enclosed basins; broken curves: energy loss at the western end; dotted curves: energy loss at the eastern end.

the basin favouring the additional energy transfer in the direction of the sink. This involves corresponding modification of tidal kinematics, i.e. the amplitude and phase pattern what, in turn, influences the characteristics of astronomical sources and sinks. Therefore the introducing of geophysical sinks may transform all the elements (items) of the energy budget.

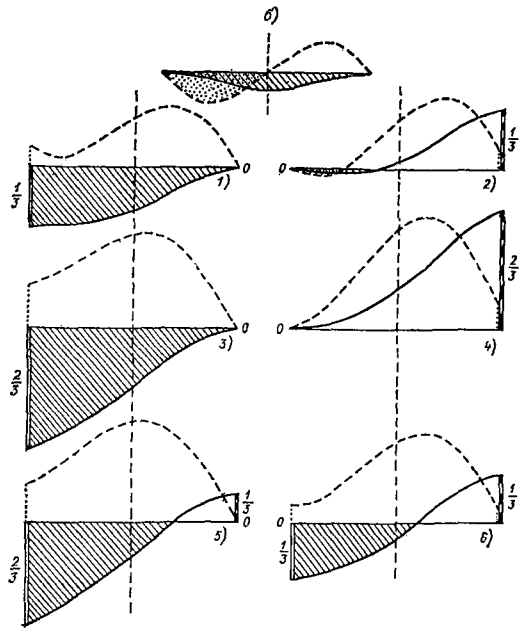

Fig. 16. Similar to Fig. 13(b) but with some conbinations of energy losses at both the ends of basins.

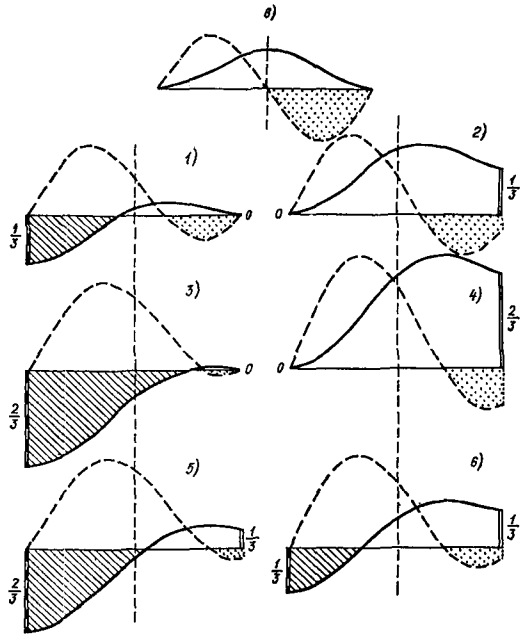

Fig. 17. Similar to Fig. 13(c) but with some combinations of energy losses.

In Figs. 16 and 17 some results are presented obtained with the boundary conditions (18) corresponding to losses equal to zero (r=1), to 1/3 (r= 0.8165) and to 2/3 (r=0.5773) of the incident wave energy admitted in various combinations for western and eastern ends. Substantial for the resulting energy flux is the position of a geophysical sink with respect to "initial" (corresponding to enclosed dissipativeless basin of same dimensions) flux direction. The sink position which originates the flux directed in the initial sense may be called positive; if otherwise-negative. Generally the positive sinks intensify the energy transfer whereas the negative sinks originate "countercurrents" in their proximity reducing the fluxes in other parts of the basin. In the last case a divergence of fluxes form an inner point is possible. Such a divergence, naturally, takes place in all cases when two sinks exist at both the ends (Nekrasov, 1990).

The influence of coastal energy loss upon astronomical items of the energy budget is also illustrated by Figs. 16 and 17. In particular, it can be seen that in some cases the geophysical sinks not only "take on themselves" some part of energy expenditures but also may stimulate the energy income by intensifying the astronomical sources whereas the astronomical sinks generally weaken. The resulting tidal movements in all mentioned cases may be interpreted as progressive-standing waves whose progressive part is reducing when approaching antiresonance. After each passing a next resonance the direction of progressive part propogation changes inversely according to the changement of the horizontal flux of energy.

REFERENCES

Godin G., 1969. Theory of exploitation of tidal energy and its application to the Bay of Fundy. *J. Fish. Res. Bd. Canada*, **26**(1): 2887-2957.

Lamb H. and Swain, L., 1915. On a tidal problem. *Phil. Mag.*, **29**(174): 737-744.

Nekrasov A.V., 1987. On the energy flux in tidal waves. *Okeanologia (Oceanology)*, **27**(6): 911-913. (in Russian).

Nekrasov A.V., 1990. Energy of ocean tides. *Leningrad Gidrometeoizdat.*: 288p. (in Russian).